

1 Topology Testing and Demographic Modeling Illuminate a Novel Speciation Pathway in the
2 Greater Caribbean Sea Following the Formation of the Isthmus of Panama.

3

4 Benjamin M. Titus^{1,2,*}, H. Lisle Gibbs², Nuno Simões^{3,4,5}, Marymegan Daly²

5

6 ¹Department of Computational Biology, University of Lausanne, Quartier Sorge, 1015

7 Lausanne, Switzerland

8 ²Department of Evolution, Ecology, and Organismal Biology, The Ohio State University,

9 Columbus, OH, USA

10 ³Facultad de Ciencias, Universidad Nacional Autonoma de Mexico-Sisal, Mexico

11 ⁴International Chair for Coastal and Marine Studies in Mexico, Harte Research Institute for Gulf
12 of Mexico Studies, Texas A&M University, Corpus Christi, TX 78412, USA

13

14 ⁵Laboratorio Nacional de Resiliencia Costera (LANRESC, CONACYT), 97356 Sisal, Yucata'n,
15 Mexico

16

17 *Correspondence to be sent to: Department of Computational Biology, University of Lausanne,

18 Quartier Sorge, 1015 Lausanne, Switzerland

19 E-mail: bentitus3@gmail.com/benjamin.titus@unil.ch

20

21 **Keywords:** Phylogeography, Coalescent Modeling, Hybrid speciation, Introgression, Crustacea,

22

23

24

25

26 **Abstract**

27 Recent genomic analyses have highlighted the prevalence of speciation with gene flow in many
28 taxa and have underscored the importance of accounting for these reticulate evolutionary
29 processes when constructing species trees and generating parameter estimates. This is especially
30 important for deepening our understanding of speciation in the sea where fast moving ocean
31 currents, expanses of deep water, and periodic episodes of sea level rise and fall act as soft and
32 temporary allopatric barriers that facilitate both divergence and secondary contact. Under these
33 conditions, gene flow is not expected to cease completely while contemporary distributions are
34 expected to differ from historical ones. Here we conduct range-wide sampling for Pederson's
35 cleaner shrimp (*Ancylomenes pedersoni*), a species complex from the Greater Caribbean that
36 contains three clearly delimited mitochondrial lineages with both allopatric and sympatric
37 distributions. Using mtDNA barcodes and a genomic ddRADseq approach, we combine classic
38 phylogenetic analyses with extensive topology testing and demographic modeling (10 site
39 frequency replicates x 45 evolutionary models x 50 model simulations/replicate = 22,500
40 simulations) to test species boundaries and reconstruct the evolutionary history of what was
41 expected to be a simple case study. Instead, our results indicate a history of allopatric divergence,
42 secondary contact, introgression, and endemic hybrid speciation driven by the final closure of the
43 Isthmus of Panama and the strengthening of the Gulf Stream Current ~3.5 million years ago. The
44 history of this species complex recovered by model-based methods that allow reticulation differs
45 from that recovered by standard phylogenetic analyses and is unexpected given contemporary
46 distributions. The geologically and biologically meaningful insights gained by our model
47 selection analyses illuminate a novel pathway of species formation that resulted from one of the
48 most biogeographically significant events in Earth's history.

49

50 **Introduction**

51 Tropical coral reefs harbor levels of biodiversity rivaled only by tropical rainforests, yet
52 do so in an environment with few obvious physical barriers to dispersal and gene flow. Although
53 speciation in the sea is not a fundamentally different biological process than on land, the extent
54 to which dispersal and gene flow drive speciation in both ecosystems can work at different scales
55 (Palumbi 1994; Vermeij and Grosberg 2010; Bowen et al. 2013; 2016; Potkamp and Fransen
56 2019). Most marine species have pelagic larvae that may raft on ocean currents for weeks,
57 connecting distant populations and resulting in large range and effective population sizes
58 (Palumbi 1994; Vermeij and Grosberg 2010; Bowen et al. 2013; 2016; Álvarez-Noriega et al.,
59 2020). Non-allopatric speciation is thus increasingly expected to play a major role in the
60 generation of tropical marine biodiversity (Choat 2006; Bowen et al. 2013; 2016). However, fast
61 moving ocean currents, expanses of deep water, and periodic episodes of sea level rise and fall
62 may act as soft or temporary allopatric barriers that can facilitate both divergence and secondary
63 contact (Quenouille et al. 2011; Cowman et al. 2013). The result is that many reef-dwelling
64 species co-occur with their close relatives in a setting where gene flow may never fully subside,
65 regardless of speciation mode.

66 That contemporary distributions may mask complex evolutionary histories creates
67 significant hurdles for understanding the origins of tropical marine biodiversity. Complicating
68 matters is that early studies of single loci (primarily mtDNA) could only capture incomplete
69 evolutionary histories, and phylogenetic approaches that employ multi-locus data often
70 concatenate data and/or deal with incongruent gene tree topologies by constructing species trees
71 that model incomplete lineage sorting (reviewed by Degnan and Rosenberg 2009). As evidence
72 continues to build in marine systems for the pervasiveness of speciation with gene flow (e.g.
73 Hurt et al. 2013; Potkamp and Fransen 2019; Simmonds et al. 2019; Titus et al. 2019a; Prada and

74 Hellberg 2020), methods that model reticulate processes are key to testing historical
75 phylogenetic hypotheses and to improving our inferences on the processes that have shaped
76 tropical marine biodiversity.

77 In the Greater Caribbean (i.e. Caribbean Sea, Bermuda, Florida Reef Tract), Pederson's
78 cleaner-shrimp *Ancylomenes pedersoni* (Chace, 1958; Fig. 1a) is a common member of coral reef
79 communities. An obligate associate of sea anemones, *A. pedersoni* primarily hosts with the
80 corkscrew anemone *Bartholomea annulata* (Briones-Fourzán et al. 2012; Mascaró et al. 2012;
81 Huebner et al. 2019). Together, these species form a hub of ecologically important cleaning
82 stations that are visited by dozens of families of coral reef fishes (e.g. Titus et al. 2015; 2017a;
83 2019b). Described as a single species throughout its range, molecular studies of mtDNA
84 barcodes have revealed two sympatric lineages along the Florida Reef Tract- one thought to be
85 endemic and one thought to be widespread in the Caribbean- and a third endemic lineage in
86 Bermuda (Titus and Daly 2015, 2017; Titus et al. 2017b). Based solely on a mtDNA
87 phylogenetic analysis with a (Florida, (Caribbean, Bermuda)) topology, Titus et al. (2017b)
88 hypothesized that a chance long distance dispersal event from the Caribbean lineage gave rise to
89 the Bermudan endemic, but were unable to make informed hypotheses regarding the origin of the
90 Florida/Caribbean divergence or whether gene flow has been important during the diversification
91 of the clade.

92 Here we conduct comprehensive range-wide sampling for *A. pedersoni* and use mtDNA
93 loci and genome-wide approaches to delimit species and disentangle the evolutionary history of
94 this species complex. We combine classic phylogenetic approaches with model-based simulation
95 methods to conduct topology testing and make demographic inferences that allow us to evaluate
96 models that invoke different modes of speciation. We find that regardless of dataset, classic
97 phylogenetic approaches combined with contemporary distributions fail to fully explain the

98 history of *A. pedersoni*. In contrast, our model-based approach highlights the complex role gene
99 flow and hybridization have played in the formation of these species and suggest that historical
100 and contemporary distributions differ. The geologically and biologically meaningful insight
101 provided by our model-based analyses ultimately allow us to identify a novel diversification
102 pathway in the Greater Caribbean following the final formation of the Isthmus of Panama.

103

104 **Materials and Methods**

105 *Sampling and DNA Extraction*

106 Whole individuals of *A. pedersoni* were collected from sea anemones by hand, using
107 SCUBA, from 14 coral reef field sites in the Greater Caribbean representing the entire
108 geographic range of the species complex (Fig. 1b; Supplementary Table S1 available on Dryad).
109 A total of 451 individuals were collected and included in this study. DNA was extracted from
110 each individual using QIAGEN DNeasy Blood & Tissue Kits, and total genomic DNA was
111 quantified (ng/ μ L) using a Qubit 2.0 fluorometer (see Supplementary Methods available on
112 Dryad).

113

114 *Sequencing and Dataset Assembly*

115 For each individual we PCR amplified and sequenced a ~650bp long fragment of mtDNA
116 from the cytochrome *c* oxidase subunit I (COI) DNA barcode (see Supplementary Methods).
117 Sequences that were newly generated for this study were deposited into GenBank (Table S1).
118 Following DNA barcoding we sequenced a subset of the 451 individuals using a double digest
119 restriction site associated DNA sequencing approach (ddRADseq). In total our ddRADseq
120 libraries included ~10-15 individuals per field locality (N = 151 individuals; see Supplementary
121 Methods; Table S2 available on Dryad). ddRADseq libraries were prepared using *Eco*-RI-HF

122 and *PstI*-HF enzymes, Illumina compatible barcodes, and a 400-800 base pair size selection
123 range. Two individuals of the closely related cleaner shrimp *Periclimenes yucatanicus* were
124 prepared and included in ddRADseq libraries as outgroup samples. Libraries were pooled and
125 sequenced across eight Illumina HiSeq 2500 lanes using single-end 100bp sequencing.

126 mtDNA barcode sequence data were assembled using Sequencher 4.9 (Gene Codes) and
127 aligned using MUSCLE (Edgar 2004) in Geneious v10.2.3 (Kearse et al. 2012). Previously
128 published COI sequences from *P. yucatanicus*, *P. rathbunae*, *P. crinoidalis*, *P. perryae*, and *P.*
129 *patae* were retrieved from GenBank included as outgroup taxa (see Supplementary Methods).

130 Raw ddRADseq reads were demultiplexed, aligned, and assembled *de novo* using the
131 program pyRAD v3.0.66 (Eaton 2014) as there is no reference genome for *A. pedersoni*. Briefly,
132 we set the clustering threshold (Wclust) to 0.90 to assemble reads into loci and a minimum
133 coverage depth of seven to call a locus (Mindepth). We required an individual sample to contain
134 at least 10,000 consensus loci after clustering, and a locus to be present in 75% of all individuals
135 to be retained in the final dataset. When more than one SNP was present at a locus, only one was
136 randomly selected to create the final unlinked SNP dataset. Because different downstream
137 analyses may or may not require outgroups, and because individual variation in sequencing
138 coverage can influence the number of recovered SNPs, we created three ddRADseq datasets: 1)
139 Full *A. pedersoni* dataset with no outgroup taxa, 2) Reduced *A. pedersoni* dataset with outgroup
140 taxa, and 3) Reduced *A. pedersoni* dataset with no outgroup taxa (see Supplementary Methods
141 and Supplementary Table S2 on Dryad). Raw ddRADseq data were deposited at the NCBI
142 Sequence Read Archive (SRA) under BioProject PRJNA693691.

143

144 *Species Delimitation and Phylogenetic Analyses*

145 To test whether Titus et al. (2017b) had identified all *A. pedersoni* species-level diversity
146 throughout the Greater Caribbean, we conducted species discovery and delimitation analyses for
147 both single locus and ddRADseq datasets. For COI DNA barcodes, we used two species
148 discovery approaches: 1) pairwise sequence divergence using the program Automatic Barcode
149 Gap Discovery (ABGD; Puillandre et al. 2012), and 2) statistical parsimony networks using the
150 program TCS v2.1 (Clement et al. 2000; see Supplementary Methods). For the full ddRADseq
151 dataset (Dataset 1), we searched for major genetic partitions in our data with genetic cluster
152 analyses using discriminate analyses of principle components (DAPC; Jombart et al. 2010) in the
153 *adegenet* package (Jombart and Ahmed 2011) in R v3.5.0 (R Core Team 2015). Next, we used
154 Bayes Factor Delimitation* (BFD*; Leache et al. 2014a) to test competing species delimitation
155 hypotheses using species trees estimated in SNAPP (Bryant et al. 2012). Specifically, we tested
156 the current taxonomy of *A. pedersoni* (i.e. one widespread species) versus species delimitations
157 recovered by single and multi-locus species discovery analyses (i.e. two and three species
158 models respectively; see Supplementary Methods).

159 Phylogenetic analyses were then conducted to reconstruct evolutionary relationships
160 among *A. pedersoni* lineages. Using single locus COI data, we used RAxML 8.9.2 (Stamatkis
161 2014) and BEAST 1.8.2 (Drummond et al. 2007) to conduct maximum likelihood (ML) and
162 Bayesian phylogenetic analyses (see Supplementary Methods). Next, we used the reduced
163 ddRADseq dataset with outgroup taxa (Dataset 2) to conduct species tree analyses using SNAPP
164 and SVDquartets (Chifman and Kubatko 2014). For both, individuals were assigned to species
165 based on the results of our species delimitation analyses (see Results). Our species tree analysis
166 was run for 1,000,000 MCMC generations in SNAPP, and trees were sampled from the posterior
167 distribution every 100 generations, 10% of which were discarded as burn-in. For SVDquartets,
168 species tree analyses were conducted in PAUP v4.0 (Swofford 2003) using the multispecies

169 coalescent model, all possible quartet combinations, and 1000 bootstrap replicates (see
170 Supplementary Methods).

171

172 *Topology testing and demographic model selection*

173 Historical and contemporary gene flow can affect species tree topologies and parameter
174 estimations (e.g., Leache et al. 2014b; Solis-Lemus et al. 2016; Jiao et al. 2020; Rannala et al.
175 2020), but species tree analyses that use the multi-species coalescent model assume gene tree
176 discordance is the result of incomplete lineage sorting (ILS) rather than gene flow. Our
177 mitochondrial gene trees and ddRADseq species trees produced conflicting, yet fully supported,
178 tree topologies, and genetic clustering analyses suggest ongoing introgression where Floridian
179 and Caribbean *A. pedersoni* lineages co-occur along the Florida Reef Tract (see Results). To
180 account for gene flow and the potential for this to bias our species tree reconstruction and
181 parameter estimates, we incorporated migration parameters into topology testing and
182 demographic model selection analyses to provide statistically supported inference on the
183 evolutionary scenarios that may have given rise to the *A. pedersoni* species complex.

184 Using the reduced ddRADseq dataset without outgroup taxa (Dataset 3), the
185 multidimensional site frequency spectrum (mSFS), and coalescent simulations in *fastsimcoal2*
186 (FSC2; Excoffier et al. 2013), we built a comprehensive set of 45 evolutionary models across all
187 possible species tree topologies that vary in the timing and directionality of migration between
188 putative species (Fig. 1c; Supplementary Fig. S1 on Dryad). We built twelve models for each
189 possible species tree topology: (Caribbean, (Florida, Bermuda)), (Florida, (Caribbean,
190 Bermuda)), and (Bermuda, (Florida, Caribbean)). Models tested for contemporary and ancestral
191 gene flow between all putative species. We also tested an additional nine evolutionary models
192 that are not explicitly reliant on hierarchical species tree topologies: three island models testing

193 all migration combinations, three models with and without migration where the Caribbean,
194 Florida, and Bermudan species diverged simultaneously forming an unresolved polytomy, and
195 three hybrid speciation models, with and without migration, where both the Caribbean and
196 Florida species provided 50% of the genetic material that gave rise to the endemic Bermudan
197 species (Fig. 1c; Supplementary Fig. S1 on Dryad).

198 To perform model selection analyses, we constructed a 3-population joint-folded mSFS
199 for putative *A. pedersoni* lineages from Florida, Caribbean, and Bermuda (see Supplementary
200 Methods). To deal with missing data and not violate the assumptions of the mSFS we conducted
201 a down sampling procedure following Smith et al. (2017; see Supplementary Methods). Ten
202 mSFS replicates were built following this approach to account for possible variation in the down
203 sampling procedure and to calculate confidence intervals for parameter estimates. We used a
204 mutation rate of $3.9e^{-9}$ substitutions per site per generation, calculated from the genome of the
205 crustacean species *Daphnia pulex* (Order Cladocera; Keith et al. 2016), to convert parameter
206 estimate values to years, effective population sizes, and per generation migration rates.
207 Parameter estimates were then further scaled by assuming 2 generations per year because *A.*
208 *pedersoni* reaches sexual maturity at ~6 months (Gilipin & Chadwick 2017). All model
209 simulations were repeated 50 times for each mSFS replicate (45 models x 10 mSFS replicates x
210 50 simulations/model/mSFS replicate = 22,500 simulations). From each of the 50 runs, the run
211 with the highest composite likelihood was selected for parameter estimation and model selection.
212 The model with the best fit to the data was selected using Akaike Information Criterion (AIC)
213 and model probabilities calculated following Burnham and Anderson (2002). Parameter
214 estimates and 95% confidence intervals were then calculated for the best fit model. All analyses
215 were conducted on the Owens cluster at the Ohio Supercomputer Center (<http://osc.edu>).

216 Finally, we conducted analysis to independently confirm model selection inferences
217 about introgression and hybridization. Specifically, we used ABBA/BABA tests to confirm
218 introgression between Floridian and Caribbean lineages along the Florida Reef Tract, and we
219 conducted hybrid detection analyses using the program HyDe (Blischak et al. 2018) to confirm
220 that the Bermudan endemic lineage received substantial genomic contributions from both
221 Floridian and Caribbean lineages (see Supplementary Methods).

222

223 **Results**

224 *Sequencing and Dataset Assembly*

225 After sequencing, alignment, and trimming, we obtained 584 bp of mtDNA *COI*
226 sequence data across 451 individuals (final alignment available on Dryad). ddRADseq library
227 preparation and sequencing resulted in a total of 300.6 million sequence reads across 153
228 individuals (151 *A. pedersoni* plus two *P. yucatanicus*; Table S2 on Dryad), 276.1 million of
229 which passed quality control filtering and were retained to create the final datasets. Of the 151 *A.*
230 *pedersoni* sequenced, 16 were not retained in the final dataset because they did not yield at least
231 10,000 consensus sequences after clustering (Table S2 on Dryad). Requiring a locus to be
232 present in 75% of all individuals resulted in final datasets of varying sizes: 1) Full *A. pedersoni*
233 dataset with no outgroup taxa (N = 135 individuals; 1232 SNPs), 2) Reduced *A. pedersoni*
234 dataset with outgroup taxa (N = 45 individuals; 2101 SNPs), and 3) Reduced *A. pedersoni*
235 dataset with no outgroup taxa (N = 43 individuals; 4673 SNPs, see Supplementary Methods and
236 Supplementary Table S2 on Dryad).

237

238 *Species Delimitation and Phylogenetic Analyses*

239 Both single locus species delimitation approaches delimit three *A. pedersoni* lineages (Fig
240 2a). No new COI lineages were recovered using range-wide sampling, although the Caribbean
241 lineage does show the classic East/West phylogeographic structure at the Mona Passage (Fig 2a).
242 Phylogenetic analyses in RAxML and BEAST recover the same fully supported mtDNA tree
243 topology (Florida, (Caribbean, Bermuda)) as Titus et al. (2017; Fig 2a).

244 Using the full ddRADseq dataset, genetic clustering analyses selected $K = 4$ as the
245 optimum partitioning scheme (Figs 2b & 2c). These clusters correspond to the species delimited
246 by COI single locus analyses: Bermuda, Florida, and Caribbean. The DAPC analyses further
247 partitioned the Caribbean species into East and West clusters, reflecting the same intraspecific
248 structuring recovered by the COI analyses. Genetic cluster analyses also demonstrate possible
249 introgression between sympatric COI lineages along the Florida Reef Tract (Fig. 2c). Four
250 individuals with COI haplotypes belonging to the Floridian Endemic lineage cluster with the
251 Western Caribbean *A. pedersoni* lineage, while four individuals belonging to the Caribbean COI
252 haplotype lineage cluster with the Floridian Endemic lineage (Fig. 2c). No individuals outside of
253 Florida differed in their COI and RADseq cluster groupings. Like the COI data, BFD* species
254 delimitation analyses picked the three species model as the best fit to the data (Table S4).

255 Although the species delimitation analyses fully agree with each other, the phylogenetic
256 analyses between single-locus and genomic data do not. Using species delimitation assignments
257 supported by BFD*, species tree analyses in both SNAPP and SVDquartets recovered fully
258 supported species tree topologies of (Caribbean, (Florida, Bermuda)) that are at odds with the
259 COI phylogenetic tree (Fig 2d).

260

261 *Topology testing and demographic model selection*

262 Demographic simulations in FSC2 and AIC model selection placed all model support on
263 a (Caribbean, (Florida, Bermuda)) tree topology, and a demographic history that indicates
264 ancestral divergence occurred in isolation, followed by contemporary introgression between
265 sympatric Caribbean and Florida species, and unidirectional contemporary gene flow from both
266 Caribbean and Florida species to Bermuda (Table 1; Fig. 3). Divergence time estimates place
267 ancestral divergence between the Caribbean lineage and the MRCA of Florida and Bermuda at
268 3.52 mya (95% CI = 3.02-4.03 mya; Supplementary Table S5), and divergence between Florida
269 and Bermuda at 0.20 mya (95% CI = 0.18-0.22 mya; Table S5). Effective population size
270 estimates were an order of magnitude larger in the Floridian species than for the Caribbean
271 species (Supplementary Table S5). Effective population sizes estimates were less than 1,000
272 individuals for the putative Bermuda species (Supplementary Table S5). Per generation
273 migration rate estimates from both putative Caribbean and Florida species to Bermuda were low
274 (Supplementary Table S5).

275 ABBA/BABA tests confirm that shared alleles between Floridian and Caribbean species
276 found along the Florida Reef Tract are the result of introgression rather than incomplete lineage
277 sorting (Supplementary Table S6). Hybrid detection analyses in HyDe indicate that the
278 Bermudan species has a significant signature of hybridization between putative Florida and
279 Caribbean species at both the population and individual level (Supplementary Table S7). HyDe
280 estimates that ~48% of the Bermudan species genome comes from the Caribbean *A. pedersoni*
281 lineage (Supplementary Table S7).

282

283 **Discussion**

284 Our evolutionary reconstruction of *Ancylomenes pedersoni* highlights the complexity of
285 the processes that can generate species-level biodiversity. While our topology tests ultimately

286 agreed with our ddRADseq species tree topology, the demographic insights gained from this
287 approach underscores the importance of using model-based analyses that account for gene flow
288 to make improved inferences beyond what is possible with classic phylogenetic methods alone.
289 Based on our best fit demographic model (Fig. 4), the Floridian and Caribbean *A. pedersoni*
290 lineages diverged ~3.5 mya without gene flow. This divergence time coincides with the final
291 closure of the Isthmus of Panama (IOP) and strengthening of the Gulf Stream, a high-volume and
292 high-velocity ocean current that originates in the Florida Straits and separates the Florida Reef
293 Tract from the Caribbean Sea (Fig. 1; Huag and Tiedemann 1998; O’Dea et al. 2016). Combined
294 with a demographic signature of introgression along the Florida Reef Tract occurring more
295 recently in the evolutionary past, we interpret the initial divergence between these lineages to
296 have occurred allopatrically across the Florida Straits, with secondary contact coming later when
297 the Caribbean lineage was able to disperse back across this barrier. Ultimately, the Gulf Stream
298 facilitated divergence and dispersal in *A. pedersoni*, and carried pelagic larvae from both
299 Floridian and Caribbean lineages >1500km to Bermuda where they hybridized and remained
300 isolated enough to warrant status as an endemic hybrid species. The evolutionary history of *A.*
301 *pedersoni* is thus far more complex than previously hypothesized by Titus et al. (2017b) and
302 highlights a novel diversification pathway that has generated species-level diversity across a
303 relatively small, but biodiverse, marine region.

304 The formation of the IOP is one of the most globally significant and heavily studied,
305 natural events in Earth’s history (reviewed by O’Dea et al. 2016). While the resulting land bridge
306 facilitated terrestrial range expansions and faunal interchange between North and South America,
307 in the oceans, the IOP severed the open seaway between the Atlantic and Pacific Oceans and sent
308 their respective communities on independent evolutionary trajectories (Knowlton et al., 1993;
309 Lessios 2008). In the Western Atlantic, the Caribbean Sea became warmer, saltier, and

310 oligotrophic, thereby facilitating major coral reef development (Lessios 2008). Although a pulse
311 of ecological speciation in scleractinian corals occurred in the 1 million years following the
312 formation of the IOP, the IOP fundamentally changed ocean circulation and global climate
313 patterns, leading directly to northern hemisphere glaciation and a period of marine extinction
314 (Budd and Johnson 1999). The repeated reduction in shallow water habitat that resulted from the
315 Pleistocene glacial cycles also decreased sea surface temperatures and drove major extinctions
316 in Caribbean corals (Budd and Johnson 1999). The result led to major ecological turnover, and
317 opportunity, in the Greater Caribbean (Budd and Johnson 1999; Budd and Klaus 2001; Prada et
318 al. 2016). In fact, while the origins of many higher-level taxonomic groups in the Caribbean can
319 be traced to major vicariant events such as the closure of the Tethys Sea and the formation of the
320 IOP (Cowman et al. 2013; Bowen et al. 2016), much of the species-level diversity that has
321 evolved within the Caribbean Sea itself appears to have originated ecologically/sympatrically
322 rather than allopatrically. Examples are wide-ranging and include reef fishes (Ruber et al. 2003;
323 Barber and Bellwood 2005; Rocha et al. 2005; Taylor and Hellberg 2005; Rocha et al. 2008;
324 Tavera et al. 2012), scleractinian corals (Weil and Knowlton 1994; Carlon and Budd, 2007;
325 Frade et al. 2010), octocorals (Lasker et al. 1983; Prada and Hellberg 2013; Prada et al. 2014;
326 Prada and Hellberg 2020), crustaceans (Knowlton and Keller 1983, 1985; Hurt et al. 2013), and
327 sea anemones (Titus et al. 2019a).

328 In contrast, allopatric speciation within the Greater Caribbean appears to be much rarer.
329 The Mona Passage between Hispaniola and Puerto Rico is identified most frequently as the major
330 phylogeographic barrier in the region separating Western and Eastern Caribbean regions, but this
331 break is almost exclusively resolved at the intraspecific level (reviewed by DeBiasse et al.,
332 2016). Hyper-restricted endemic taxa have been only been described occasionally from the
333 Meso-American Barrier Reef and Southern Caribbean (Colin, P. 2002; Taylor and Hellberg

334 2005; 2006; Hurt et al. 2013; D'Aloia et al. 2017). Much of the allopatric diversity that arises in
335 the Tropical Western Atlantic comes via dispersal from the Greater Caribbean to Brazil where
336 major freshwater runoff from the Amazon basin creates a major barrier to gene flow between
337 regions (reviewed by Bowen et al. 2016). This is despite the fact that the formation of the IOP
338 deflected equatorial currents in the Atlantic northwards through the Caribbean Sea and into the
339 Gulf of Mexico where the current loops clockwise, meanders slightly, and then is pulled
340 downwards by gravity through the narrow Florida Straits, strengthening the Gulf Stream, which
341 can move 30 million cubic meters of water per second at velocities up to 2.5 m/s (Fig 1).
342 Although a number of phylogeographic studies also identify the Florida Straits as an important
343 intraspecific phylogeographic barrier, to our knowledge, no examples have demonstrated that
344 speciation has occurred across this barrier, let alone coincided with the formation of the IOP and
345 led to downstream endemic hybrid speciation. Instead, the Gulf Stream is often discussed as a
346 means of explaining the relative homogeneity between Bermudan and Caribbean marine
347 communities, and the subsequent low rates of Bermudan endemism although though the nearest
348 coral reef system is >1500 kilometers away (reviewed by Titus et al. 2017b).

349 Our data thus uncover a novel example of the evolutionary consequences the formation
350 of the Isthmus of Panama has had on marine biodiversity. Our study is a particularly important
351 example for marine evolutionary biologists demonstrating the complexity of the geological,
352 biological, and physical oceanographic processes that generate biodiversity on coral reefs
353 reinforcing that ocean currents can act as temporal allopatric barriers and downstream dispersal
354 pathways simultaneously. Finally, although introgressive hybridization is not uncommon in
355 marine systems, true hybrid speciation is rarely documented, and the importance of these
356 reticulate evolutionary processes are poorly understood (reviewed by Arnold and Fogarty 2009).
357 The results of our study argue strongly that methods that model gene flow and reticulate

358 processes be included regularly into systematic studies in the sea, particularly on the shallow
359 evolutionary timescales we have worked with here.

360

361 **Acknowledgements**

362 We thank Erich Bartels, Annelise del Rio, Jose Diaz, Dan Exton, Natalie Hamilton, Alex Hunter,
363 Anna Klompen Jason Macrander, Spencer Palombit, Stephen Ratchford, Jill Titus, Cory Walter,
364 Eric Witt, Clay Vondriska, and the Operation Wallacea dive staff for assistance in the field and
365 laboratory. Alonso Delgado assisted with ddRADseq analyses, and Jordan Satler and Megan
366 Smith provided valuable advice on simulation analyses and model selection. Bellairs Research
367 Station, the Bermuda Institute of Ocean Science, Cape Eleuthera Institute, CARMABI, Coral
368 View Dive Center, Gerace Research Centre, the Honduran Coral Reef Foundation, Mote Marine
369 Laboratory, Smithsonian Tropical Research Institute, and the University of the Virgin Islands
370 provided valuable logistical support. Specimens were collected under permits: SE/A-88- 15,
371 PPF/DGOPA-127/14, CZ01/9/9, FKNMS-2012-155, SAL-12-1432A-SR, STT037-14, 140408,
372 MAR/FIS/17, 19985, and N. PPF/DGOPA-295/17. This research was supported by National
373 Science Foundation Doctoral Dissertation Improvement Grant DEB-1601645 and Florida Fish
374 and Wildlife Conservation Commission awards to B.M.T. & M.D. Operation Wallacea,
375 American Philosophical Society, International Society for Reef Studies Graduate Fellowship,
376 PADI Foundation Grant, American Museum of Natural History Lerner Gray Funds, and The
377 Ohio State University Presidential Fellowship provided funding to B.M.T. Field work in Mexico
378 was financially supported by CONACyTCB-2012-01-177293, CONABIO NE018, and the Harte
379 Research Institute assigned to NS. Additional funding was provided through the Trautman Fund
380 of The OSU Museum of Biological Diversity, The Ohio State University, and the National
381 Science Foundation DEB-1257796 to MD.

382

383

384 **References**

- 385 Álvarez-Noriega, M., Burgess, S.C., Byers, J.E., Pringle, J.M., Wares, J.P. and Marshall, D.J.,
386 2020. Global biogeography of marine dispersal potential. *Nature Ecology &*
387 *Evolution*, 4(9), pp.1196-1203.
- 388
- 389 Arnold, M.L. and Fogarty, N.D., 2009. Reticulate evolution and marine organisms: the final
390 frontier? *International Journal of Molecular Sciences*, 10(9), pp.3836-3860.
- 391
- 392 Barber, P.H. and Bellwood, D.R., 2005. Biodiversity hotspots: evolutionary origins of
393 biodiversity in wrasses (Halichoeres: Labridae) in the Indo-Pacific and new world
394 tropics. *Molecular Phylogenetics and Evolution*, 35(1), pp.235-253.
- 395
- 396 Blischak, P.D., Chifman, J., Wolfe, A.D. and Kubatko, L.S., 2018. HyDe: a Python package for
397 genome-scale hybridization detection. *Systematic Biology*, 67(5), pp.821-829.
- 398
- 399 Bowen, B.W., Rocha, L.A., Toonen, R.J. and Karl, S.A., 2013. The origins of tropical marine
400 biodiversity. *Trends in Ecology & Evolution*, 28(6), pp.359-366.
- 401
- 402 Bowen, B.W., Gaither, M.R., DiBattista, J.D., Iacchei, M., Andrews, K.R., Grant, W.S., Toonen,
403 R.J. and Briggs, J.C., 2016. Comparative phylogeography of the ocean
404 planet. *Proceedings of the National Academy of Sciences*, 113(29), pp.7962-7969.
- 405
- 406 Briones-Fourzán, P., Pérez-Ortiz, M., Negrete-Soto, F., Barradas-Ortiz, C. and Lozano-Álvarez,
407 E., 2012. Ecological traits of Caribbean sea anemones and symbiotic
408 crustaceans. *Marine Ecology Progress Series*, 470, pp.55-68.
- 409
- 410 Bryant, D., Bouckaert, R., Felsenstein, J., Rosenberg, N.A. and RoyChoudhury, A., 2012.
411 Inferring species trees directly from biallelic genetic markers: bypassing gene trees in a
412 full coalescent analysis. *Molecular Biology and Evolution*, 29(8), pp.1917-1932.
- 413
- 414 Budd, A.F. and Johnson, K.G., 1999. Origination preceding extinction during late Cenozoic
415 turnover of Caribbean reefs. *Paleobiology*, 25(2), pp.188-200.
- 416
- 417 Budd, A.F. and Klaus, J.S., 2001. The origin and early evolution of the *Montastraea* “annularis”
418 species complex (Anthozoa: Scleractinia). *Journal of Paleontology*, 75(3), pp.527-545.
- 419
- 420 Burnham, K.P. and Anderson, D.R., 2002. Model selection and multimodal inference: A
421 practical information theoretic approach. 2nd ed. New York, NY: Springer
- 422
- 423 Carlon, D.B. and Budd, A.F., 2002. Incipient speciation across a depth gradient in a scleractinian
424 coral? *Evolution*, 56(11), pp.2227-2242.
- 425

- 426 Chace, F.A. Jr. (1958) A new shrimp of the genus *Periclimenes* from the West Indies.
427 *Proceedings of the Biological Society of Washington*, 71, 125–130.
428
- 429 Choat, J.H., 2006. Phylogeography and reef fishes: bringing ecology back into the
430 argument. *Journal of Biogeography*, 33(6), pp.967-968.
431
- 432 Chifman, J. and Kubatko, L., 2014. Quartet inference from SNP data under the coalescent
433 model. *Bioinformatics*, 30(23), pp.3317-3324.
434
- 435 Clement, M., Posada, D.C.K.A. and Crandall, K.A., 2000. TCS: a computer program to estimate
436 gene genealogies. *Molecular Ecology*, 9(10), pp.1657-1659.
437
- 438 Colin, P.L., 2002. A new species of sponge-dwelling *Elacatinus* (Pisces: Gobiidae) from the
439 western Caribbean. *Zootaxa*, 106(1), pp.1-7.
440
- 441 Cowman, P.F. and Bellwood, D.R., 2013. Vicariance across major marine biogeographic
442 barriers: temporal concordance and the relative intensity of hard versus soft
443 barriers. *Proceedings of the Royal Society B: Biological Sciences*, 280(1768),
444 p.20131541.
445
- 446 D'Aloia, C.C., Bogdanowicz, S.M., Harrison, R.G. and Buston, P.M., 2017. Cryptic genetic
447 diversity and spatial patterns of admixture within Belizean marine
448 reserves. *Conservation Genetics*, 18(1), pp.211-223.
449
- 450 DeBiasse, M.B., Richards, V.P., Shivji, M.S. and Hellberg, M.E., 2016. Shared
451 phylogeographical breaks in a Caribbean coral reef sponge and its invertebrate
452 commensals. *Journal of Biogeography*, 43(11), pp.2136-2146.
453
- 454 Degnan, J.H. and Rosenberg, N.A., 2009. Gene tree discordance, phylogenetic inference and the
455 multispecies coalescent. *Trends in Ecology & Evolution*, 24(6), pp.332-340.
456
- 457 Drummond, A.J. and Rambaut, A., 2007. BEAST: Bayesian evolutionary analysis by sampling
458 trees. *BMC Evolutionary Biology*, 7(1), pp.1-8.
459
- 460 Eaton, D.A., 2014. PyRAD: assembly of de novo RADseq loci for phylogenetic
461 analyses. *Bioinformatics*, 30(13), pp.1844-1849.
462
- 463 Edgar, R.C., 2004. MUSCLE: multiple sequence alignment with high accuracy and high
464 throughput. *Nucleic Acids Research*, 32(5), pp.1792-1797.
465
- 466 Excoffier, L., Dupanloup, I., Huerta-Sánchez, E., Sousa, V.C. and Foll, M., 2013. Robust
467 demographic inference from genomic and SNP data. *PLoS Genet*, 9(10), p.e1003905.
468
- 469 Frade, P.R., Reyes-Nivia, M.C., Faria, J., Kaandorp, J.A., Luttikhuisen, P.C. and Bak, R.P.M.,
470 2010. Semi-permeable species boundaries in the coral genus *Madracis*: introgression in
471 a brooding coral system. *Molecular Phylogenetics and Evolution*, 57(3), pp.1072-1090.
472

- 473 Haug, G.H. and Tiedemann, R., 1998. Effect of the formation of the Isthmus of Panama on
474 Atlantic Ocean thermohaline circulation. *Nature*, 393(6686), pp.673-676.
475
- 476 Huebner, L.K., Shea, C.P., Schueller, P.M., Terrell, A.D., Ratchford, S.G. and Chadwick, N.E.,
477 2019. Crustacean symbiosis with Caribbean sea anemone *Bartholomea annulata*:
478 occupancy modeling, habitat partitioning, and persistence. *Marine Ecology Progress
479 Series*, 631, pp.99-116.
480
- 481 Hurt, C., Silliman, K., Anker, A. and Knowlton, N., 2013. Ecological speciation in
482 anemone-associated snapping shrimps (*Alpheus armatus* species complex). *Molecular
483 Ecology*, 22(17), pp.4532-4548.
484
- 485 Gilpin, J.A. and Chadwick, N.E., 2017. Life-history traits and population structure of Pederson
486 cleaner shrimps *Ancylomenes pedersoni*. *The Biological Bulletin*, 233(3), pp.190-205.
487
- 488 Jiao, X., Flouri, T., Rannala, B. and Yang, Z., 2020. The impact of cross-species gene flow on
489 species tree estimation. *Systematic Biology*, 69(5), pp.830-847.
490
- 491 Jombart, T., Devillard, S. and Balloux, F., 2010. Discriminant analysis of principal components:
492 a new method for the analysis of genetically structured populations. *BMC
493 Genetics*, 11(1), p.94.
494
- 495 Jombart, T. and Ahmed, I., 2011. adegenet 1.3-1: new tools for the analysis of genome-wide
496 SNP data. *Bioinformatics*, 27(21), pp.3070-3071.
497
- 498 Kearse, M., Moir, R., Wilson, A., Stones-Havas, S., Cheung, M., Sturrock, S., Buxton, S.,
499 Cooper, A., Markowitz, S., Duran, C. and Thierer, T., 2012. Geneious Basic: an
500 integrated and extendable desktop software platform for the organization and analysis of
501 sequence data. *Bioinformatics*, 28(12), pp.1647-1649.
502
- 503 Keith, N., Tucker, A.E., Jackson, C.E., Sung, W., Lledó, J.I.L., Schridder, D.R., Schaack, S.,
504 Dudycha, J.L., Ackerman, M., Younge, A.J. and Shaw, J.R., 2016. High mutational
505 rates of large-scale duplication and deletion in *Daphnia pulex*. *Genome Research*, 26(1),
506 pp.60-69.
507
- 508 Knowlton, N. and Keller, B.D., 1983. A new, sibling species of snapping shrimp associated with
509 the Caribbean sea anemone *Bartholomea annulata*. *Bulletin of marine science*, 33(2),
510 pp.353-362.
511
- 512 Knowlton, N. and Keller, B.D., 1985. Two more sibling species of alpheid shrimps associated
513 with the Caribbean sea anemones *Bartholomea annulata* and *Heteractis lucida*. *Bulletin
514 of Marine Science*, 37(3), pp.893-904.
515
- 516 Knowlton, N., Weigt, L.A., Solorzano, L.A., Mills, D.K. and Bermingham, E., 1993. Divergence
517 in proteins, mitochondrial DNA, and reproductive compatibility across the Isthmus of
518 Panama. *Science*, 260(5114), pp.1629-1632.
519

- 520 Lasker, H.R., Gottfried, M.D. and Coffroth, M.A., 1983. Effects of depth on the feeding
521 capabilities of two octocorals. *Marine Biology*, 73(1), pp.73-78.
522
- 523 Leaché, A.D., Fujita, M.K., Minin, V.N. and Bouckaert, R.R., 2014. Species delimitation using
524 genome-wide SNP data. *Systematic Biology*, 63(4), pp.534-542.
525
- 526 Leaché, A.D., Harris, R.B., Rannala, B. and Yang, Z., 2014. The influence of gene flow on
527 species tree estimation: a simulation study. *Systematic Biology*, 63(1), pp.17-30.
528
- 529 Lessios, H.A., 2008. The great American schism: divergence of marine organisms after the rise
530 of the Central American Isthmus. *Annual Review of Ecology, Evolution, and*
531 *Systematics*, 39, pp.63-91.
532
- 533 Mascaró, M., Rodríguez-Pestaña, L., Chiappa-Carrara, X. and Simões, N., 2012. Host selection
534 by the cleaner shrimp *Ancylomenes pedersoni*: Do anemone host species, prior
535 experience or the presence of conspecific shrimp matter? *Journal of Experimental*
536 *Marine Biology and Ecology*, 413, pp.87-93.
537
- 538 O’Dea, A., Lessios, H.A., Coates, A.G., Eytan, R.I., Restrepo-Moreno, S.A., Cione, A.L.,
539 Collins, L.S., De Queiroz, A., Farris, D.W., Norris, R.D. and Stallard, R.F., 2016.
540 Formation of the Isthmus of Panama. *Science Advances*, 2(8), p.e1600883.
541
- 542 Palumbi, S.R., 1994. Genetic divergence, reproductive isolation, and marine speciation. *Annual*
543 *Review of Ecology, Evolution, and Systematics*, 25(1), pp.547-572.
544
- 545 Potkamp, G. and Fransen, C.H., 2019. Speciation with gene flow in marine
546 systems. *Contributions to Zoology*, 88(2), pp.133-172.
547
- 548 Prada, C. and Hellberg, M.E., 2013. Long prereproductive selection and divergence by depth in a
549 Caribbean candelabrum coral. *Proceedings of the National Academy of*
550 *Sciences*, 110(10), pp.3961-3966.
551
- 552 Prada, C., McIlroy, S.E., Beltrán, D.M., Valint, D.J., Ford, S.A., Hellberg, M.E. and Coffroth,
553 M.A., 2014. Cryptic diversity hides host and habitat specialization in a gorgonian-algal
554 symbiosis. *Molecular Ecology*, 23(13), pp.3330-3340.
555
- 556 Prada, C., Hanna, B., Budd, A.F., Woodley, C.M., Schmutz, J., Grimwood, J., Iglesias-Prieto, R.,
557 Pandolfi, J.M., Levitan, D., Johnson, K.G. and Knowlton, N., 2016. Empty niches after
558 extinctions increase population sizes of modern corals. *Current Biology*, 26(23),
559 pp.3190-3194.
560
- 561 Prada, C. and Hellberg, M., 2020. Speciation-by-depth on coral reefs: sympatric divergence with
562 gene flow or cryptic transient isolation? *Journal of Evolutionary Biology*.
563
- 564 Puillandre, N., Lambert, A., Brouillet, S. and Achaz, G., 2012. ABGD, Automatic Barcode Gap
565 Discovery for primary species delimitation. *Molecular Ecology*, 21(8), pp.1864-1877.
566

- 567 Quenouille, B., Hubert, N., Bermingham, E. and Planes, S., 2011. Speciation in tropical seas:
568 allopatry followed by range change. *Molecular Phylogenetics and Evolution*, 58(3),
569 pp.546-552.
570
- 571 R Core Team 2015. R: A language and environment for statistical computing. Vienna, Austria: R
572 Foundation for Statistical Computing. <https://wwwR-project.org/>
573
- 574 Rannala, B., Edwards, S.V., Leaché, A. and Yang, Z., 2020. The multi-species coalescent model
575 and species tree inference. *Phylogenetics in the Genomic Era*, pp.3.3:1-3.3:21.
576
- 577 Rocha, L.A., Robertson, D.R., Roman, J. and Bowen, B.W., 2005. Ecological speciation in
578 tropical reef fishes. *Proceedings of the Royal society B: Biological Sciences*, 272(1563),
579 pp.573-579.
580
- 581 Rüber, L., Van Tassell, J.L. and Zardoya, R., 2003. Rapid speciation and ecological divergence
582 in the American seven-spined gobies (Gobiidae, Gobiosomatini) inferred from a
583 molecular phylogeny. *Evolution*, 57(7), pp.1584-1598.
584
- 585 Simmonds, S.E., Chou, V., Cheng, S.H., Rachmawati, R., Calumpong, H.P., Mahardika, G.N.
586 and Barber, P.H., 2018. Evidence of host-associated divergence from coral-eating snails
587 (genus *Coralliophila*) in the Coral Triangle. *Coral Reefs*, 37(2), pp.355-371.
588
- 589 Smith, M.L., Ruffley, M., Espíndola, A., Tank, D.C., Sullivan, J. and Carstens, B.C., 2017.
590 Demographic model selection using random forests and the site frequency
591 spectrum. *Molecular Ecology*, 26(17), pp.4562-4573.
592
- 593 Solís-Lemus, C., Yang, M. and Ané, C., 2016. Inconsistency of species tree methods under gene
594 flow. *Systematic Biology*, 65(5), pp.843-851.
595
- 596 Stamatakis, A., 2014. RAxML version 8: a tool for phylogenetic analysis and post-analysis of
597 large phylogenies. *Bioinformatics*, 30(9), pp.1312-1313.
598
- 599 Swofford, D.L., 2004. Paup 4.0 for Macintosh: Phylogenetic analysis using parsimony (software
600 and user's book for Macintosh)
601
- 602 Tavera, J.J., Acero, A., Balart, E.F. and Bernardi, G., 2012. Molecular phylogeny of grunts
603 (Teleostei, Haemulidae), with an emphasis on the ecology, evolution, and speciation
604 history of New World species. *BMC Evolutionary Biology*, 12(1), p.57.
605
- 606 Taylor, M.S. and Hellberg, M.E., 2005. Marine radiations at small geographic scales: speciation
607 in neotropical reef gobies (*Elacatinus*). *Evolution*, 59(2), pp.374-385.
608
- 609 Taylor, M.S. and Hellberg, M.E., 2006. Comparative phylogeography in a genus of coral reef
610 fishes: biogeographic and genetic concordance in the Caribbean. *Molecular*
611 *Ecology*, 15(3), pp.695-707.
612

- 613 Titus, B.M. and Daly, M., 2015. Fine-scale phylogeography reveals cryptic biodiversity in
614 Pederson's cleaner shrimp, *Ancylomenes pedersoni* (Crustacea: Caridea: Palaemonidae),
615 along the Florida Reef Tract. *Marine Ecology*, 36(4), pp.1379-1390.
616
- 617 Titus, B.M. and Daly, M., 2017. Specialist and generalist symbionts show counterintuitive levels
618 of genetic diversity and discordant demographic histories along the Florida Reef
619 Tract. *Coral Reefs*, 36(1), pp.339-354.
620
- 621 Titus, B.M., Daly, M. and Exton, D.A., 2015. Temporal patterns of Pederson shrimp
622 (*Ancylomenes pedersoni* Chace 1958) cleaning interactions on Caribbean coral
623 reefs. *Marine Biology*, 162(8), pp.1651-1664.
624
- 625 Titus, B.M., Vondriska, C. and Daly, M., 2017a. Comparative behavioural observations
626 demonstrate the 'cleaner' shrimp *Periclimenes yucatanicus* engages in true symbiotic
627 cleaning interactions. *Royal Society Open Science*, 4(4), p.170078.
628
- 629 Titus, B.M., Palombit, S. and Daly, M., 2017b. Endemic diversification in an isolated
630 archipelago with few endemics: an example from a cleaner shrimp species complex in
631 the Tropical Western Atlantic. *Biological Journal of the Linnean Society*, 122(1), pp.98-
632 112.
633
- 634 Titus, B.M., Blischak, P.D. and Daly, M., 2019a. Genomic signatures of sympatric speciation
635 with historical and contemporary gene flow in a tropical anthozoan (Hexacorallia:
636 Actiniaria). *Molecular Ecology*, 28(15), pp.3572-3586.
637
- 638 Titus, B.M., Daly, M., Vondriska, C., Hamilton, I. and Exton, D.A., 2019b. Lack of strategic
639 service provisioning by Pederson's cleaner shrimp (*Ancylomenes pedersoni*) highlights
640 independent evolution of cleaning behaviors between ocean basins. *Scientific
641 Reports*, 9(1), pp.1-9.
642
- 643 Vermeij, G.J. and Grosberg, R.K., 2010. The great divergence: when did diversity on land
644 exceed that in the sea? *Integrative and Comparative Biology*, 50(4), pp.675-682.
645
- 646 Weil, E. and Knowlton, N., 1994. A multi-character analysis of the Caribbean coral *Montastraea*
647 *annularis* (Ellis and Solander, 1786) and its two sibling species, *M. faveolata* (Ellis and
648 Solander, 1786) and *M. franksi* (Gregory, 1895). *Bulletin of Marine Science*, 55(1),
649 pp.151-175.
650

651

652

653

654

655

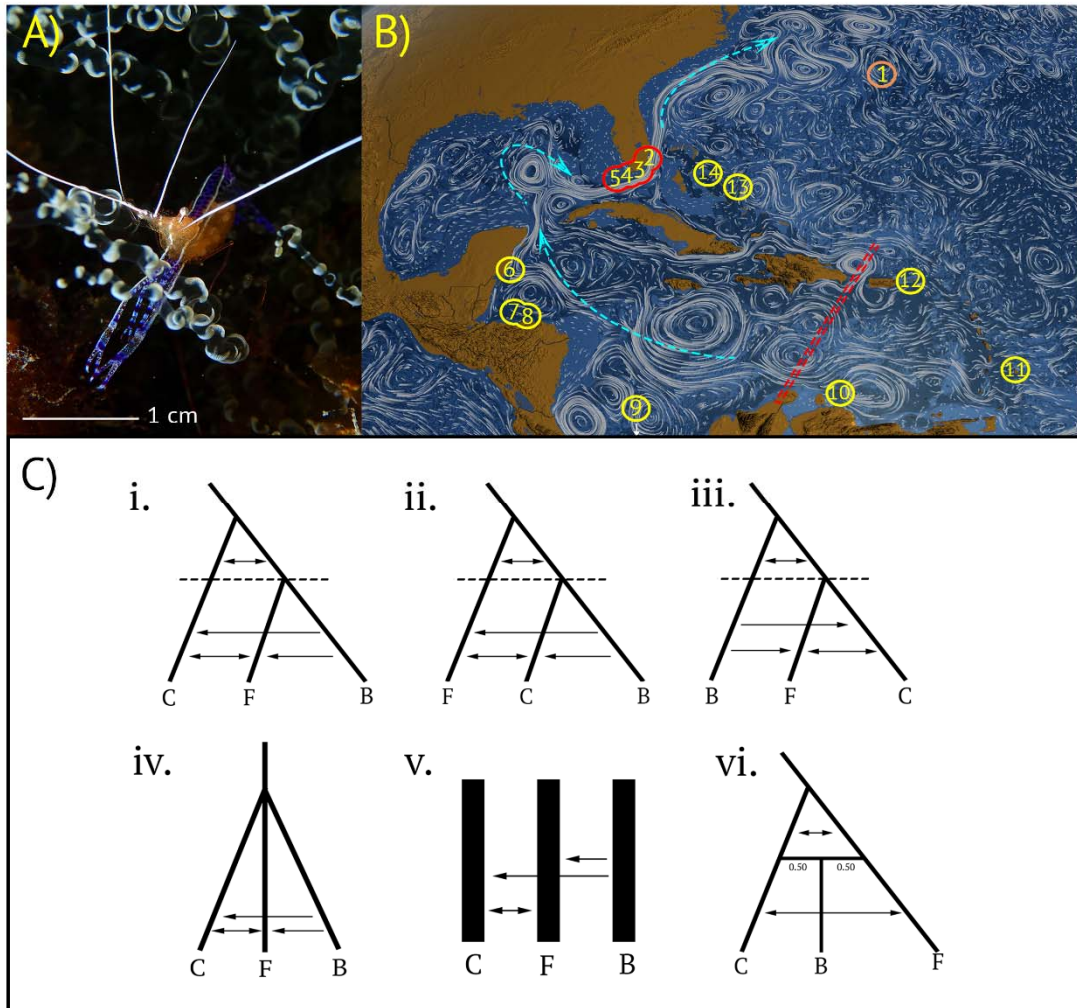
656

657

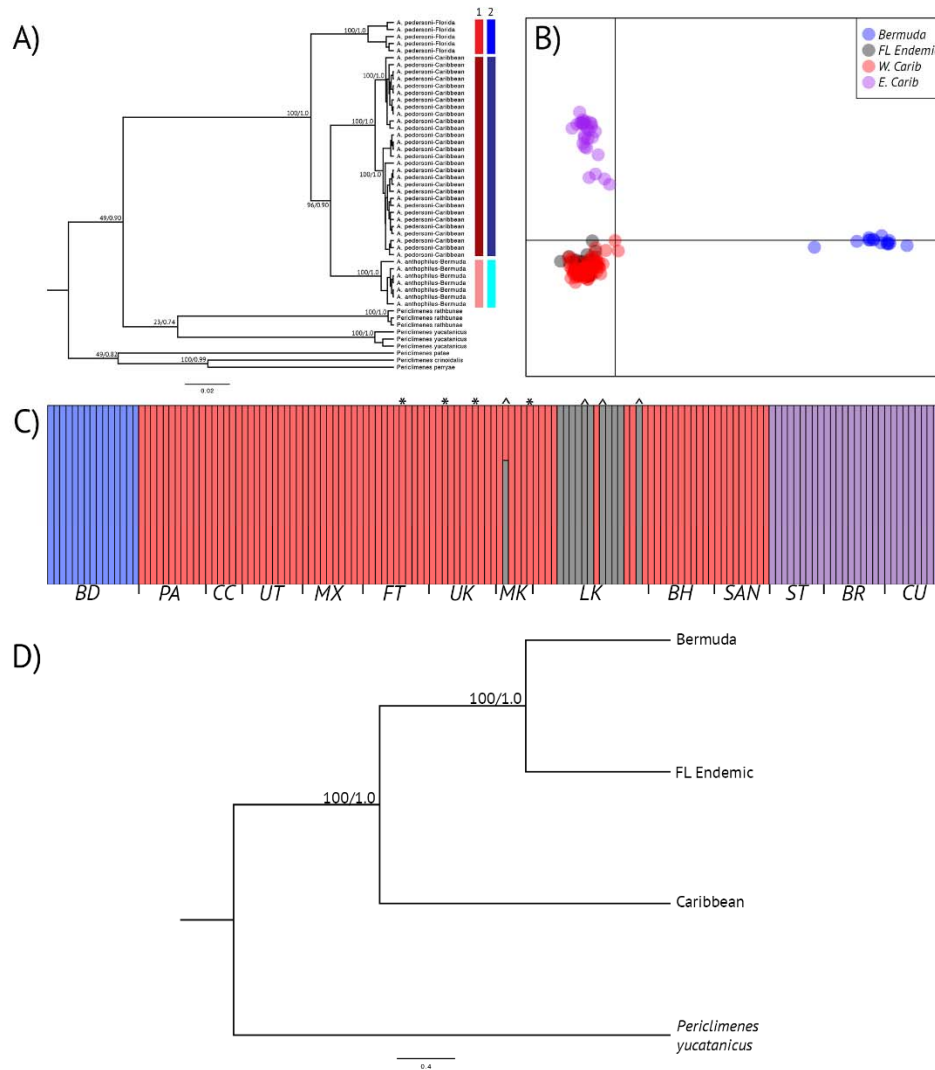
658 Table 1. Akaike Information Criterion results for models simulated in FSC2 for the *Ancylomenes pedersoni* species
 659 complex. Model name refers to variants of those depicted and described in Figure 2. k = number of parameters in the
 660 model, AIC = Akaike Information Criterion, Δ_i = change in AIC scores, and w_i = Akaike weights. Prefixes on model
 661 names refer to variation in model type and tree topology: A = ((Caribbean, (Florida, Bermuda)); B = ((Florida,
 662 (Caribbean, Bermuda)); C = ((Bermuda, (Caribbean, Florida)); Isl = Island Model; Hyb = Hybridization model; Sim
 663 = simultaneous divergence model. Models are listed according to their AIC rank and the highest ranked model is
 664 highlighted.

Model	k	Log (P)	AIC	Δ_i	Model Likelihood	w_i
i-Mod10	11	-22603.84	45229.67	0	1	1
ii-Mod6	10	-22676.34	45372.69	143.01	8.8e-32	8.8e-32
ii-Mod10	11	-22752.57	45527.15	297.48	2.5e-65	2.5e-65
iii-Mod11	14	-22999.99	46027.99	798.32	4.4e-174	4.4e-174
i-Mod11	12	-23010.73	46045.46	815.79	7.1e-178	7.1e-178
ii-Mod5	11	-23208.93	46439.85	1210.17	1.6e-263	1.6e-263
ii-Mod9	12	-23219.90	46463.79	1234.11	1.0e-268	1.0e-268
ii-Mod11	12	-23288.88	46601.75	1372.08	1.1e-298	1.1e-298
Sim-Mod3	9	-23311.22	46640.44	1410.76	4.5e-307	4.5e-307
ii-Mod7	9	-23322.72	46663.43	1433.75	0	0
iii-Mod7	11	-23331.81	46685.61	1455.93	0	0
iii-Mod6	11	-23350.94	46723.87	1494.19	0	0
ii-Mod3	10	-23421.51	46863.02	1633.34	0	0
ii-Mod2	9	-23503.47	47024.93	1795.25	0	0
ii-Mod4	10	-23510.66	47041.32	1811.64	0	0
Isl-Mod3	6	-23567.15	47146.29	1916.61	0	0
iii-Mod10	8	-23617.00	47249.99	2020.31	0	0
Isl-Mod2	7	-23625.89	47265.79	2036.11	0	0
iii-Mod9	9	-23681.36	47380.72	2151.04	0	0
ii-Mod8	8	-23742.41	47500.83	2271.14	0	0
i-Mod12	9	-23742.79	47543.59	2313.90	0	0
ii-Mod12	9	-23796.70	47611.40	2381.72	0	0
Hyb-Mod2	10	-23804.42	47628.84	2399.16	0	0
iii-Mod8	9	-23821.71	47661.43	2431.75	0	0
ii-Mod1	7	-23910.76	47835.53	2605.85	0	0
Hyb-Mod3	11	-24004.63	48031.26	2801.58	0	0
Sim-Mod2	7	-24593.07	49200.14	3970.46	0	0
Hyb-Mod1	8	-24598.03	49212.06	3982.38	0	0
iii-Mod3	10	-24691.93	49403.87	4174.19	0	0
Sim-Mod1	5	-24723.30	49456.61	4226.93	0	0
iii-Mod5	10	-24742.51	49505.02	4275.34	0	0
i-Mod7	9	-24766.59	49551.18	4321.50	0	0
i-Mod4	10	-24773.07	49566.14	4336.46	0	0
i-Mod5	11	-24789.54	49601.07	4371.39	0	0
i-Mod9	12	-24792.60	49609.20	4379.52	0	0
i-Mod2	9	-24796.43	49610.87	4381.19	0	0
iii-Mod4	9	-24807.98	49633.96	4404.28	0	0
iii-Mod2	8	-24809.91	49635.82	4406.14	0	0
i-Mod3	10	-24809.13	49638.27	4408.59	0	0
i-Mod8	8	-24816.92	49638.27	4420.16	0	0
iii-Mod12	8	-24825.62	49667.25	4437.57	0	0
i-Mod6	10	-24832.44	49684.87	4455.19	0	0
iii-Mod1	7	-24856.22	49726.44	4496.76	0	0
i-Mod1	7	-24919.15	49852.29	4622.61	0	0
Isl-Mod1	6	-25386.13	50784.27	5554.59	0	0

665

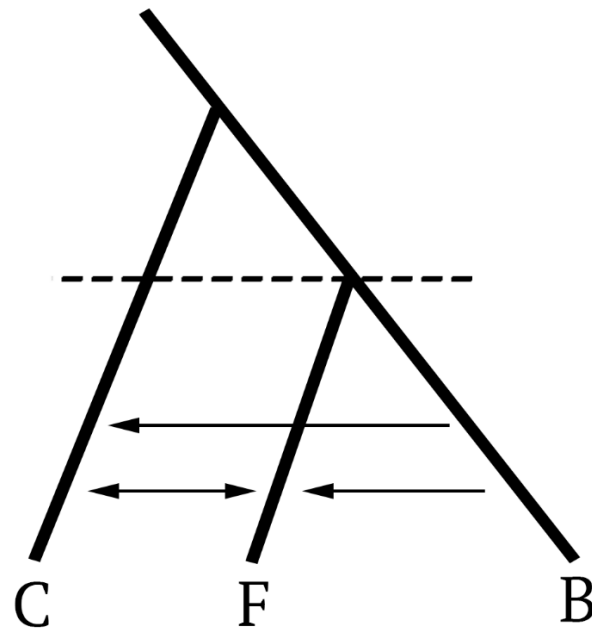


666
667 Figure 1. A) Representative image of *Ancylomenes pedersoni*. B) Field sampling localities in the Tropical
668 Western Atlantic 1) Bermuda 2) Ft. Lauderdale, FL, USA, 3) Upper Keys, FL, USA, 4) Middle Keys, FL,
669 USA, 5) Lower Keys, FL, USA, 6) Mahahual, Mexico, 7) Utila, Honduras, 8) Cayos Cochinos, Honduras,
670 9) Bocas del Toro, Panama, 10) Curacao, 11) Barbados, 12) St. Thomas, US Virgin Islands, 13) San
671 Salvador, Bahamas, 14) Eleuthera, Bahamas. Field site circle color indicates geographic range of each
672 putative species: orange = endemic Bermudan lineage, red = endemic Floridian plus Caribbean lineages,
673 and yellow = Caribbean lineage. Ocean currents depicted by white stylized lines. Current strength
674 corresponds to white line density and length. Directionality of major ocean currents depicted by light blue
675 dashed lines. Map background and ocean currents visualization from NASA/Goddard Space Flight Center
676 Scientific Visualization Studio. Ocean currents visualized from current data collected from June 2005 –
677 December 2007. Double red dashed line demarcates the major phylogeographic break in the Caribbean.
678 C) Examples of the most parameter rich models used in *fastsimcoal2* simulations. i-iii) Isolation-
679 migration models on a fixed species tree topology with variation in the timing and directionality of
680 migration. iv) Isolation-migration models with simultaneous divergence between putative species. v)
681 Island models. vi) Hybrid speciation model where the Bermudan lineage represents a 50/50 hybrid
682 between Caribbean and Floridian species. Hybrid models were built with and without ancestral and
683 contemporary gene migration. C = Caribbean, F = Florida, B = Bermuda. Arrows represent migrations
684 events in the coalescent (i.e. backwards in time). In total, 45 models were built and simulated by
685 considering all pairwise combinations of gene flow between species (see main text)



686
 687 Figure 2. A) Results from cytochrome *c* oxidase subunit (*COI*) phylogenetic gene tree reconstruction of
 688 *Ancylomenes pedersoni*. Node labels represent bootstrap and posterior probability values from RAxML
 689 and BEAST. Colored bars represent single locus species delimitation results from 1) Automatic barcode
 690 gap detection (ABGD) and 2) Parsimony haplotype network reconstruction (TCS). B) Scatterplot
 691 depicting K = 4 genetic clusters for *A. pedersoni* throughout the Tropical Western Atlantic using double
 692 digest Restriction Site Associated DNA sequencing (ddRADseq). The best clustering scheme was
 693 determined by discriminant analysis of principal components (DAPC) and Bayesian Information
 694 Criterion. C) Bar plot depicting K = 4 genetic clusters for *A. pedersoni* ddRADseq data using DAPC
 695 analyses: Bermuda (blue), Florida Endemic (Gray), Western Caribbean (Red), and Eastern Caribbean
 696 (purple). * denotes introgressed individuals with FL endemic COI haplotypes. ^ denotes introgressed
 697 individuals with Western Caribbean COI haplotypes. Sample locality codes are as follows: BD (Bermuda),
 698 PA (Bocas del Toro, Panama), CC (Cayos Cochinos, Honduras), UT (Utila, Honduras), MX (Mahauhal,
 699 Mexico), FT (Ft. Lauderdale, FL, USA), UK (Upper Keys, FL, USA), MK (Middle Keys, FL, USA), LK
 700 (Lower Keys, FL, USA), BH (Eleuthera, Bahamas), SAN (San Salvador, Bahamas), ST (St. Thomas, US
 701 Virgin Islands), BR (Barbados), CU (Curacao, Netherlands Antilles). D) ddRADseq species tree
 702 reconstruction of the three *A. pedersoni* lineages as delimited by BFD*. Node values represent bootstrap
 703 values and posterior probabilities as determined by SVDquartets and SNAPP.
 704

705
706
707



708

709 Figure 4. Best fit topology and evolutionary model for the *Ancylomenes pedersoni* species complex.
710 Arrows represent migration events in the coalescent (i.e. backwards in time).